Automated injection for High-Power Fiber Amplifiers

Ted Conley
McQuaid Jesuit High School
LLE Advisor: Dr. Jake Bromage
Summer 2009

Abstract

New ytterbium-doped fiber amplifiers are enabling femtosecond systems to produce gigawatt peak powers [1]. A critical development is the fiber itself. New photonic crystal fibers (PCF) have large single-mode effective areas (<2300 μm^2) and high pump absorptions (30 dB/m), raising the power at which nonlinear pulse distortion occurs. The nature of the design, however, has some limitations. Single-mode operation is only possible if the fiber is kept straight. Therefore, instead of the typical 0.25-mm diameter fibers that can be coiled and fusion spliced, the large-mode-area PCF fibers are 1.6-mm diameter rods. One consequence is that the pump and signal beams must be injected into the fiber using free-space optics. The output beam quality of the amplifier degrades with significant misalignment at injection [2]. For this project, control software was written to (a) observe the amount of misalignment at the signal injection, (b) calculate the required correction, and (c) move the signal beam by issuing commands to a motorized mirror. Closed-loop control was demonstrated with correction times of roughly 10 seconds, and corrected for deviations as large as the fiber core diameter.

1. Introduction

1.1 Photonic-crystal fiber amplifiers

Fiber amplifiers have unique thermal advantages over solid-state amplifiers due to their geometry. Their large aspect ratio (long length to small diameter) provides a large surface area to active volume ratio, which improves heat dissipation. The geometry also provides efficient amplification due to the long path lengths available for absorbing the pump light. However, the aspect ratio is less advantageous at higher peak powers. When high energy pulses propagate down the fiber, the intensity of the light can become much larger than in other solid-state amplifiers because of the small area of the fiber mode. At sufficiently high intensities, nonlinear distortion of the pulse occurs in the fiber [3] . For short-pulse amplifiers, the dominant nonlinearity is due to instantaneous modification of the refractive index of the glass by the time-varying intensity of the pulse. This in turn modifies the phase of the pulse. Hence, this effect is called 'self-phase modulation' (SPM).

One way to compare the threshold for SPM between different fiber amplifiers is by their nonlinearity coefficient, γ [3]

$$\gamma = \frac{n_2 \omega_0}{c A_{\text{eff}}} \qquad (1)$$

where n_2 is the nonlinear index of the glass (2.4 x 10^{-16} W/cm^2), ω_0 is the optical frequency, and c is the speed of light. A_{eff} is the critical parameter that fiber designers can use to improve the power-handling capabilities of the fiber. Doubling A_{eff} approximately doubles the length over which a pulse can propagate for the same amount of nonlinear distortion. Alternatively, twice the power can be propagated over the same length of fiber.

New fiber designs such as the photonic crystal fiber (PCF) have been introduced to increase A_{eff} . PCFs have a double-cladding structure created by the presence of two arrays of air holes that run

the length of the fiber. The presence of air within the fiber lowers the average refractive index of the regions containing the arrays, permitting confinement of light by total internal reflection. The structure of the fiber used for this project is displayed in Fig. 1 and was studied in detail by Schmidt *et al.* [4].

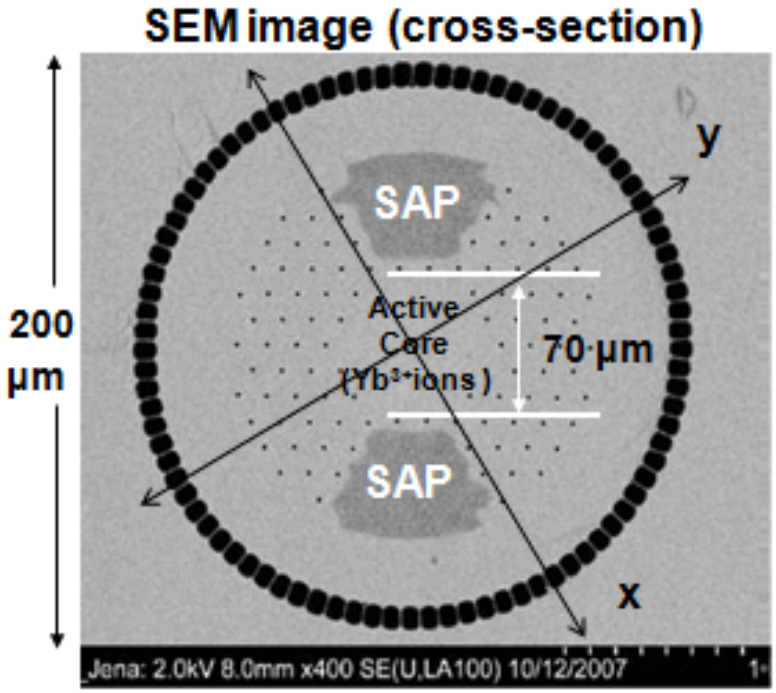

Fig. 1: Scanning electron microscope image of a cross section of the photonic crystal fiber amplifier displaying the multiple arrays of air holes used for radiation confinement. Labels indicate differing regions of the fiber and their dimensions. The actual orientation of the fiber is indicated as well; the x axis denotes the horizontal orientation and the y axis the vertical.

Three types of structures are used here. The first is an circular ring of air holes. This creates a large refractive index difference that can confine light even when it propagates at large angles down the fiber (i.e., with high numerical aperture, NA). This light is guided by this ring up to a half-angle of 37°, which corresponds to a numerical aperture of 0.6. The ring is used to confine the amplifier pump, 976-nm light from multimode-fiber pigtailed diodes, to a 200-µm diameter region down the fiber. Tight confinement of the pump light ensures efficient pumping of the ytterbium ions that dope the 70-µm-diameter region in the core of the fiber. The pump absorption of 30 dB/m is approximately 6 times

higher than found in standard single-mode fiber amplifiers, and allows the fiber length to be reduced to less than a meter.

The second structure consists of a hexagonal matrix of smaller air holes. Their size is 1.1 μm and they are spaced 11 μm apart. Their role is to lower the average index of the region surrounding the core of the fiber, to guide the signal light at 1030 to 1050 nm. In contrast to the strong guiding of the pump light, the guiding of the signal light is extremely weak (NA ≈ 0.02, or a maximum half-angle of 1.1°). This is done to ensure that only the lowest-order mode, the fundamental mode, can successfully propagate down the fiber. Higher-order modes, which would severely degrade the beam profile of the amplified signal, leak out of the fiber structure, and therefore are reduced at the output of the fiber amplifier. The advantage of this design is that A_{eff} for the signal is 2300 μm^2, 100 times larger than the effective area of standard singlemode amplifiers, and corresponds to a mode-field diameter of 55 μm. The disadvantage of this weak-guiding approach is that the fiber cannot be bent or the fundamental mode will also leak out of the fiber. Therefore, the fiber is rigidly encased in a 1.6-mm diameter glass rod.

The third type of structure is the two boron-doped stress-applying parts (SAP) that are used to create stress birefringence within the fiber. This is a standard technique for changing the polarization properties of the fiber [4]. The SAPs modify the refractive index seen by the signal. If the signal is polarized vertically (along a line connecting the SAPs), the mode is confined. If, however, the orthogonal polarization is launched, the mode is not confined and the light leaks out of the fiber. In this way, the polarization of the input signal is preserved at the output.

1.2 Application: Ultra-broadband Front-End Project

A new project is underway at the Laboratory for Laser Energetics (LLE) to create an ultra-broadband front end (UFE) for upgrading OMEGA EP to produce extremely short pulses (approximately 30 fs) with high energies (>500 J). High-power PCF amplifiers are being used in the prototype front end

to produce the seed pulses required for the upgrade, which must have approximately 200 nm of bandwidth, centered at 910 nm. The PCF amplifier is part of a fiber chirped-pulse amplifier system that creates 10-μJ pulses at a 1-MHz repetition rate. These pulses are used to (a) generate white-light continuum using a sapphire plate, and (b) amplify the continuum in a noncollinear optical parametric amplifier. (For more details, see [5]). Key requirements of the PCF amplifier are good beam quality and long term stability. This project addressed both of these requirements by actively correcting the signal beam injection at the input to the amplifier.

1.3 Experimental set-up

Figure 2 shows the experimental system. In the UFE prototype, the fiber rests on a metal v-shaped mount that is mounted on the optical table at two points.

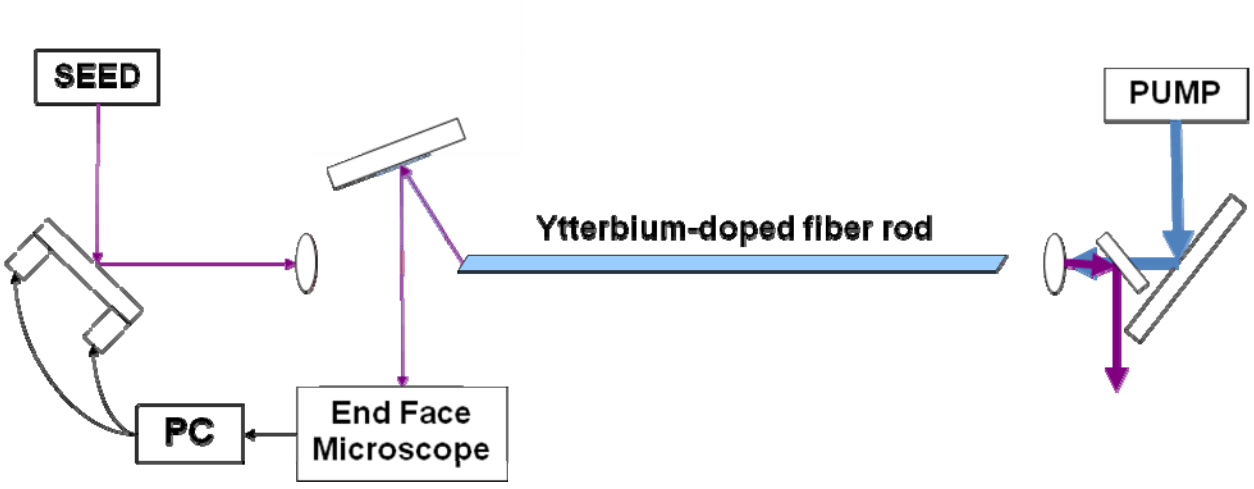

Fig. 2: Diagram of the experimental set-up. The box labeled SEED represents previous optical elements that create the seed pulse. Ovals represent lenses, and plain white rectangles represent mirrors. The blue parallelogram represents the fiber itself.

The blue arrows represent the path taken by the pump light into the fiber, while the purple arrows denote the seed and eventually the output laser beam. The relative powers are indicated by the thickness of the arrows. The signal power is 0.45 W at input and increases to 16 W at output. The pump light input power is 60 W. The seed beam is reflected off the mirror on the left, to which actuators are attached to provide control. The beam then passes through a lens which focuses the light to a point for

injection. Some of the signal light is reflected into the end face microscope (EFM) objective along with much of the excess pump light. The signal gains energy along the length of the fiber, exits, disperses, and is refocused by a second lens. Figure 3 displays an overhead photograph of the actual optical array.

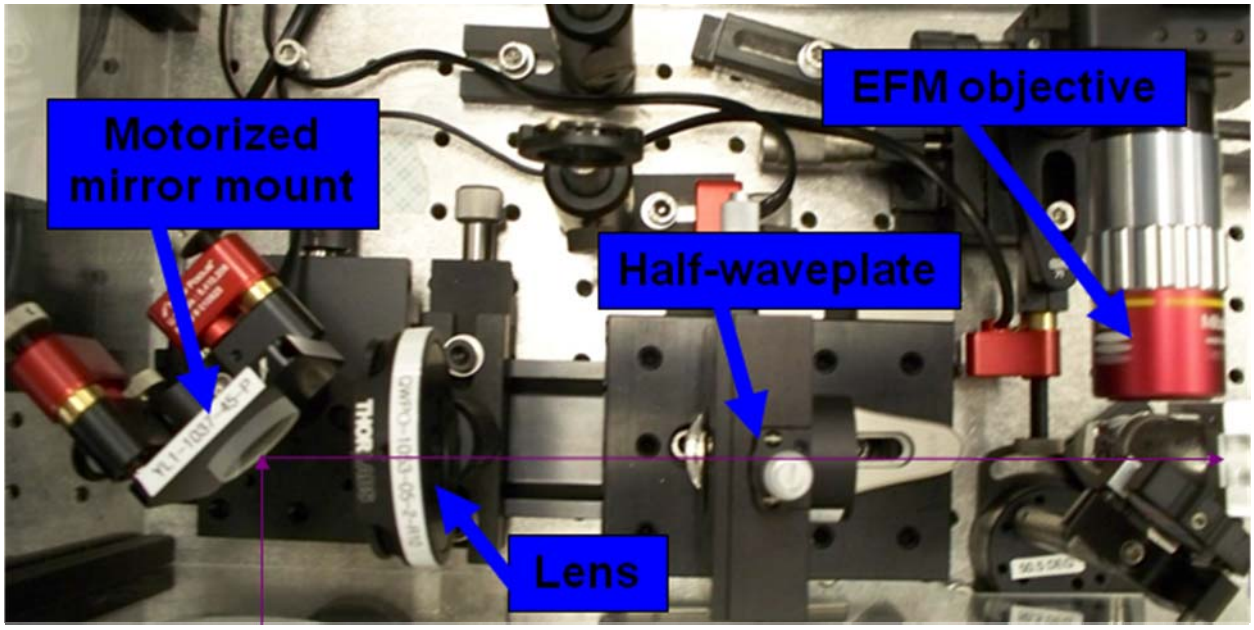

Fig. 3 A top view of the optical components leading up to the fiber including the motorized mirror mount, lens, and half-waveplate which locks the signal polarization for injection.

1.4 Statement of the problem

The properties of the PCF, while advantageous for short-pulse amplification, raise issues that are not typical for fiber amplifiers.. The rigid rod design means that traditional fusion splicing techniques cannot be used to integrate the PCF into a system. Instead the pump and signal light must be launched into the fiber through free-space injection. The performance of the amplifier is sensitive to error in the injection alignment. If the misalignment is of the order of the mode-field diameter (55 μm), coupling into the fundamental mode of the fiber is severely reduced and, therefore, the output of the amplifier is lower by more than an order of magnitude. Less severe misalignment also causes problems. Higher-order modes (HOM's) that have different mode profiles and propagation velocities can also be launched if the injection is offset from center. Although the PCF is designed not to propagate such modes, the fiber length is short enough (0.8 m) that some fraction of the HOM can still be present at the output of

the amplifier. Interference between the fundamental mode (LP_{01}) and the HOM's distorts the beam profile. The distortion can be significant even when the relative powers differ more than an order of magnitude because it is an interference effect [6]. Injection offsets of 30% of the mode-field diameter (15 μm) can increase the amount of the LP_{11} HOM from -18 dB to -13 dB [2].

These issues would be less detrimental if the fiber input was held in a fixed position to within a few microns. Heating by the pump, however, causes a number of competing effects that change the position of the center of the active core due to thermal expansion. These effects were reduced by adding a chilled-water cooling system in the fiber mount. Nonetheless, since the fiber rests in a v-shaped mount, as the diameter of the fiber expands, the target injection site changes position. The displacement observed is not in one dimension directly upwards, as viewed in a traditional x-y plane through the fiber face, but generally has an x component as well. Figure 4 shows the displacement in both the x and y dimensions over more than one hour.

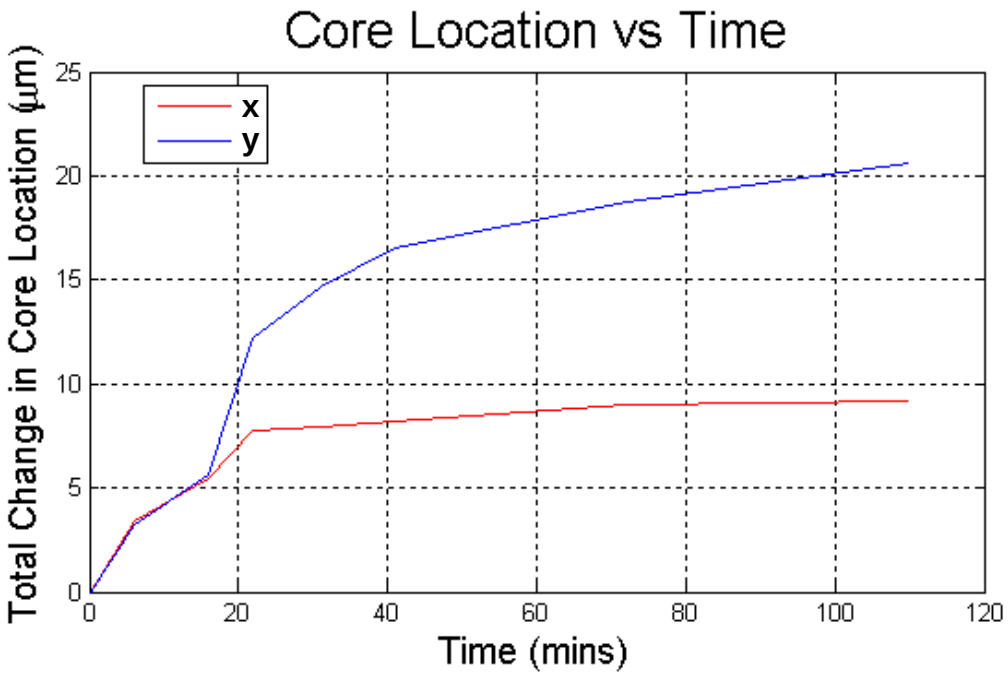

Fig. 4: Graph of the cumulative change in core position over time as the system heats up. Red and blue lines graph total displacement in the X and Y dimensions respectively, both in the positive direction on a traditional co-ordinate plane.

This unidirectional movement may be due to the orientation of the active core within the fiber and the position of the fiber in relation to the fiber mount. The doped core is not in the exact center of this specific fiber and the stress applying parts (SAP) are actually askew in this fiber. An alternative hypothesis is that the diameter of the fiber itself expands, and due to the v-shaped mount the active core rises as operation progresses (see Fig. 5).

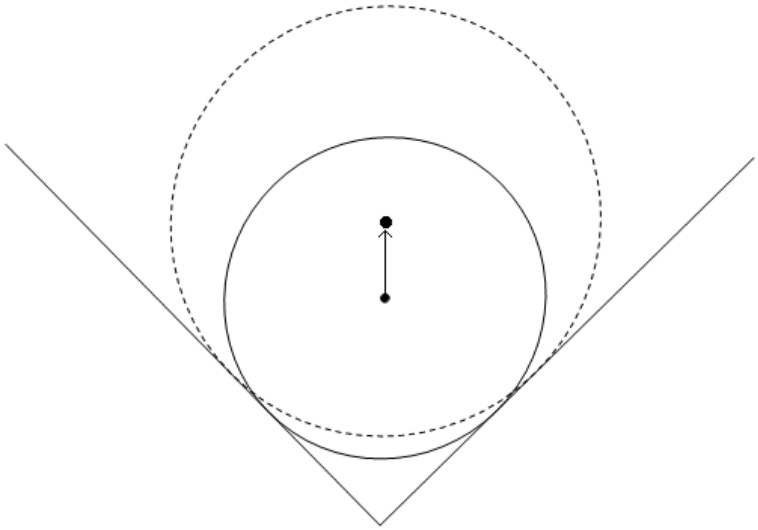

Fig. 5: Diagram of one hypothesis for how thermal expansion of the fiber creates one vector component of misalignment. (Scales are exaggerated for clarity).

Another theory is that the mount itself absorbs much of the heat dissipated from the fiber. Since the mount is fixed to an optical table at two points, the thermal expansion of the mount causes it to bow upwards at the center. The fiber is not entirely rigid and conforms to the new shape of the fiber mount causing the end face of the fiber to change position and orientation, thus additionally dislocating the target injection site.

The maximum rate of change of the position of the target injection site can be estimated from Fig. 4. When the system is first turned on the rate of change is the highest at approximately

0.5 μm/min. This continuous change in the active core location required constant manual adjustments of the signal injection. To simplify operation, it was decided that the adjustment process should be automated.

2. Methods

2.1 Automated Alignment Approach

The approach to developing a system that would automatically align the beam with the target injection site required three main tasks:

1. The system must be able to acquire some sort of readable data about the relative positions of the ideal signal injection site and the signal location. The data needs to be readily available, required by the desired real time function of the system, and easily processed.
2. The system must be able to evaluate the acquired data and calculate the injection error between signal location and ideal signal location.
3. The system must then be able to transfer this error value into commands sent to some external control system that will mechanically correct the injected signal beam.

2.2 Implementation

The data is acquired in the form of an image created by the combination of pump and signal light captured by an end-face microscope (EFM) (see Fig. 2). The end face of the fiber that the signal is injected into is polished to an angle of about 4°, reflecting approximately 4% of the signal light to the EFM. (The 4° angle is required so that the amplifier does not lase from reflections between its end faces). A substantial amount of excess pump light is also captured by the EFM pickoff, providing a background by illuminating the pump core with the exception of the SAP's. The superimposition of these two light sources creates a distinct image such as that shown in Fig. 6(a); the circular signal region has the highest intensity, followed by the pump core without the SAP's at a significantly lower intensity, and finally the SAPs and the region surrounding the core are dark. The image is recorded by a CCD camera as a 640 x 480 matrix of intensity values and later evaluated for the locations of the signal and

target core. This entire process is handled using LabVIEW, a program that uses a graphical user interface (GUI) that represents data flow as a circuit to create virtual instruments (VIs) for data acquisition and instrument control. LabVIEW's IMAQ functions allowed simple communication with the EFM's CCD for frequent image snapping and continuous evaluation.

MATLAB, a high-level matrix manipulation software package, was used to evaluate the EFM image. MATLAB also supports LabVIEW integration, so once created, the MATLAB algorithm could be easily used as a function within the overall VI. The image is processed in two discrete segments, one to locate the signal within the image and another more complex process to locate the target injection site. Fundamental to both processes is the calculation of the centroid of the intensity distribution. Similar to calculating the center of mass of an object, the centroid calculation factors in intensity and distance from an axis to calculate the centroid coordinate for one dimension. When applied to both axes, this calculation yields a point denoting the "center of intensity" of a matrix of intensity values. The centroid calculation was applied to a number of sub-images, obtained by manipulations of the original intensity array to separate certain components.

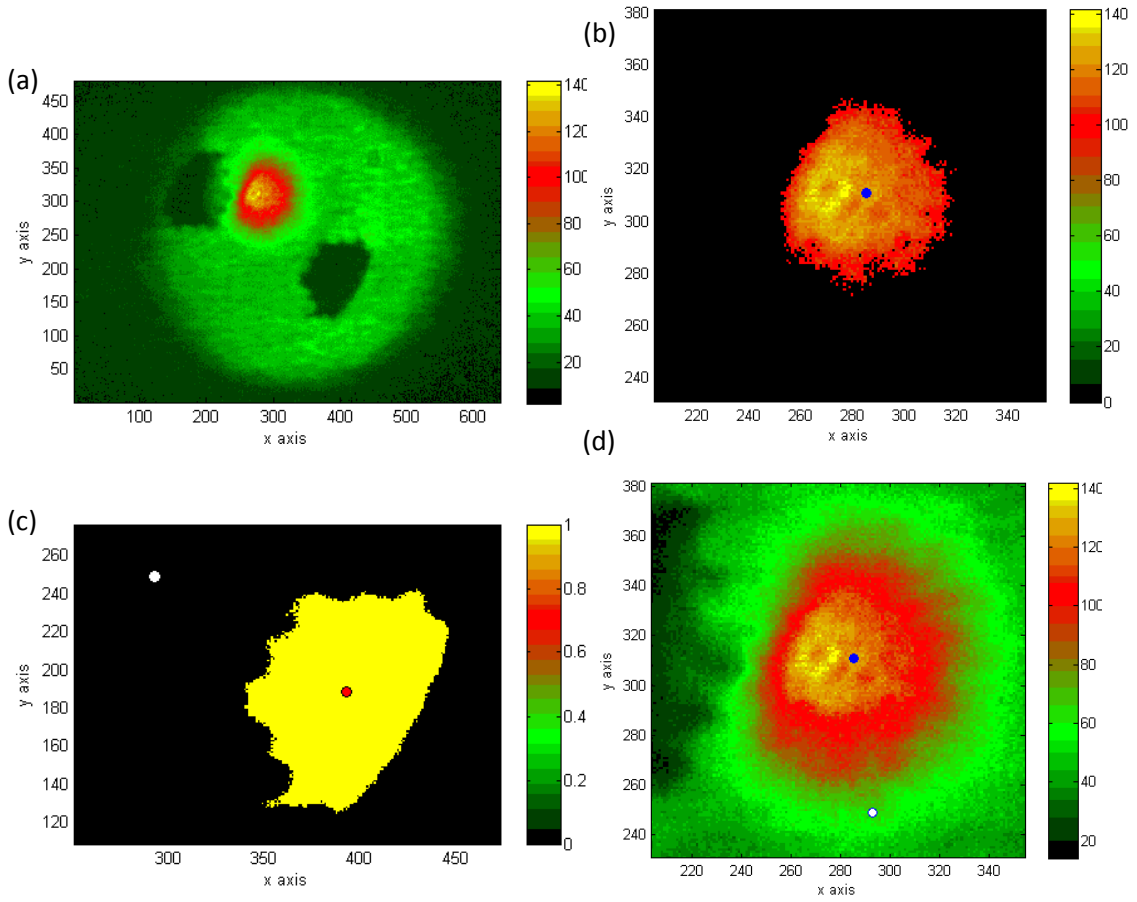

Fig. 6: Series of images representing the process used to calculate the misalignment at injection. Sub-image (a) displays the original image derived from the unaltered matrix of intensity values obtained from the CCD. Sub-image (b) shows the product of the signal locations process, a smaller region including only the signal with the centroid indicated with a blue marker. Sub-image (c) shows the product of the target location process, a smaller region with the centroids of the SAP and ideal injection site indicated. Sub-image (d) shows the combination of the calculated actual and ideal injection locations.

A number of the sub-images used in calculations are displayed in Fig. 6. The sub-image used to find the location of the signal beam is calculated by simply applying a strict threshold to the original image, [see Fig. 6 (a)]. "Thresholding" an image entails setting all values below a certain level, a threshold value, to zero, creating a separate image consisting of only the pixels of highest intensity. When a threshold is applied to the original image, the resulting matrix includes only the signal pulse and occasionally a hot pixel separate from that beam. Since the centroid calculation is fairly sensitive to pixels a large distance from the main distribution, it is performed a number of times, each time narrowing down the region of

interest (ROI). The program calculates a centroid, uses that point as a reference to establish a smaller ROI, which contains only the signal with no extra space for extraneous pixels, to yield the image labeled shown in Fig. 6 (b). The algorithm then calculates the centroid of this smaller image only. This allows the program to avoid the influence of extreme value pixels when calculating the true center of the signal beam.

The process used to calculate the injection target uses the SAP's. These reference point are more difficult to locate. The original image is binarized; that is, any value above a certain arbitrary level is set to a value of one, and every value below that level is set to zero. This creates an image depicting only the outline of the fiber, with the SAPs as blank spots within that outline. This image is used to find an extremely rough value for the center of the fiber. Each row or column is summed, and since every pixel now has the same value the row with the highest sum is taken to be a diameter of the circle, or very close, and used as the y-value for the center of the circle. The same is done for the columns to obtain the x coordinate. This point is not reliable enough to use for the target of injection but it is stable enough for the program to use it as a reference point and generally locate an SAP based on relative positions. An ROI is established based on the rough center to zoom in on the SAP and the sub-image is re-inverted to give the region defining the SAP the positive values. The centroid of this region is calculated, and that point is used to establish a more accurate ROI. The centroid of the second ROI containing the SAP, which creates the image labeled Fig. 6 (c), is taken to be the center of the SAP. The position of the ideal injection site relative to the SAP location is known, so the location of the injection site is obtained from the stable SAP center location. Once the signal and target locations are known the error is calculated by subtracting the coordinates of the target from the coordinates of the signal, yielding the change necessary to align the two, as shown in Fig. 6 (d).

Once the program obtains these error values it must convert them into commands usable by the motors that adjust the path of the signal beam. The mount for the final mirror contains two picomotor

actuators (New Focus, model 8807) that change the pointing of the signal with an angular resolution of 0.7 μrad in both directions. After the mirror, the signal beam passes through the focusing lens, and the angular shifts are changed to lateral translations at the input face of the PCF. The error values, measured in pixels, are converted to motor commands, measured in steps, using ratios obtained from a calibration process executed at the initiation of the VI in which the program moves the motors various numbers of steps and records the change in signal location based on those movements. The changes and motor counts are plotted and the slope of the resulting least-squares fit is used for the ratio. This procedure is used for each direction in each dimension and also records ratios for the change in signal location in one dimension created by a motor movement in the other dimension, yielding eight total ratios for conversion**.** The VI then uses the built-in linear algebra functions in LabVIEW to convert the error values to the necessary motor counts. In order to avoid counterproductive movement the VI runs a number of Boolean checks and prevents the calculation of any motor commands that would move the signal further from the target. A possible solution to positive x error could include more positive x direction movement, and then the negative correction, so the VI tests error values and prevents such corrections. The obtained motor counts are then inserted into prefabricated commands prepared to be compatible with the driver used to communicate with the actuators and sent. The motors adjust the mirror, correcting the error, and the process repeats.

3. Discussion

3.1 Performance

The system's utility is defined by two characteristics, speed of tracking and the maintenance of accuracy over time. The developed VI exceeds requirements for both criteria. The fiber drift is slow at approximately 0.5 μm/min, as shown in Fig. 4. The maximum frequency of adjustment (approximately once per second) by the VI is more than enough to keep the signal within an acceptable error range; the operational speed was artificially slowed by the inclusion of a delay so that the actuators were not

adjusting too frequently. The system also maintains error values well within the empirically determined error range of ±5 µm. Figure 7 shows a graph displaying a typical trial of the performance of the system in regards to speed and accuracy. The system reacts very quickly and maintains error values for both x and y within the accepted range, denoted by bold black lines.

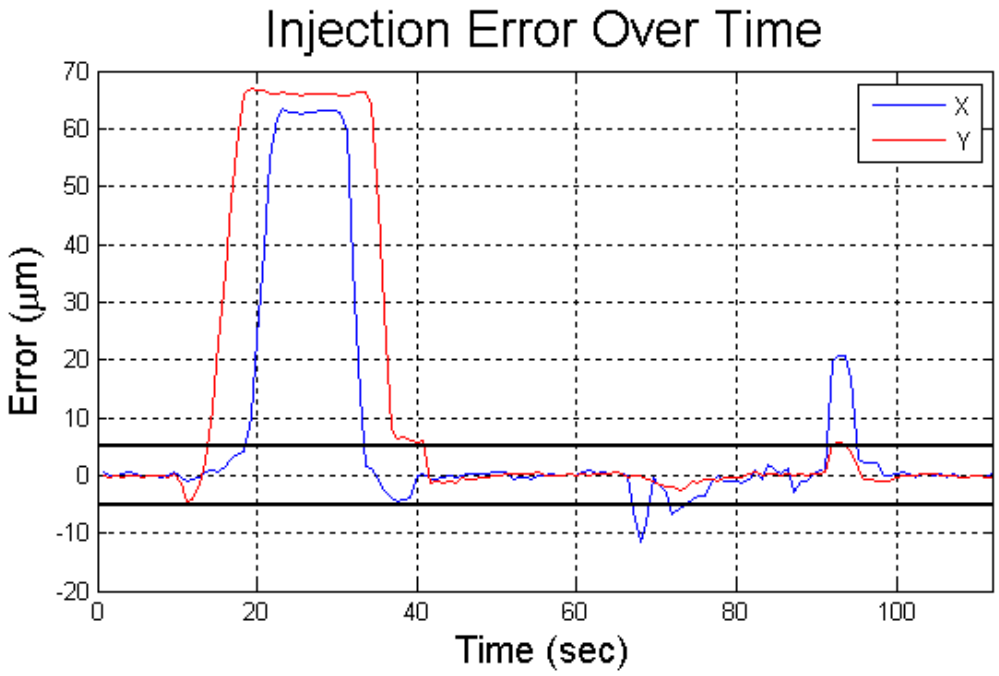

Fig. 7: Graph of injection error versus time for a test run of the software's tracking capabilities. The significant displacement spikes around 20, 70, and 90 seconds are the result of manually induced misalignment to test the program's tracking capability.

3.2 Precautions

One concern with automated alignment is always the risks associated with system failure. In this application, the risks are significant. If the signal is not injected into the fiber core, the available gain of the amplifier is not saturated, increasing the possibility that it will lase, producing a short, intense pulse through self pulsation [7,8]. These pulses can be intense enough that they can irreversibly damage the PCF and the optical components that come before and after it. If the program were to incorrectly analyze an image of the fiber end and divert the signal beam away from the fiber face entirely while the pump was operating at full power the optical system could be damaged. The VI

contains a number of precautions to guard against this. The system runs Boolean checks on all outgoing motor commands, disallowing any action that attempts to move the motors more than a previously set distance limit. If the program attempts such a dangerous command all autonomous tracking is halted, the user is notified, and manual control is restored.

4. Conclusion

The rigid structure of PCFs that provides their nonlinearity and thermal advantages also prevents the use of traditional splicing techniques, necessitating the use of free-space injection. The high-power operation of the PCF results in the dissipation of high amounts of excess heat, causing the location of the optimal injection site to shift during operation. A software program was designed to analyze images taken from an end face microscope to monitor and correct free-space injection. After performance tests, the system was found to exceed requirements for speed and accuracy.

5. Acknowledgements

Many thanks to my supervisor Dr. Jake Bromage for all of his guidance over the course of the program, and to Dr. Craxton for selecting me for the program in the first place.

6. References

[1] J. Limpert, *et al.* , 'High Repetition Rate Gigawatt Peak Power Fiber Laser Systems: Challenges, Design, and Experiment,' *IEEE Journal of Selected Topics in Quantum Electronics,* **15**, 159 (2009)

[2] J. Bromage, *et al.* 'Optimizing injection into large-mode-area photonic crystal fiber amplifiers by spatially resolved spectral interferometry', presented at the *Conference for Lasers and Electro-Optics*, paper CWD3, Baltimore, MD (2009)

[3] G. Agrawal, *Nonlinear Fiber Optics*, 2nd ed. (Academic, San Diego, 1995)

[4] O. Schmidt, *et al.* 'Single-polarization ultra-large-mode-area Yb-doped photonic crystal fiber,' Opt. Express **16**, 3918 (2008)

[5] J. Bromage, *et al*. 'High-Resolution Spatio-Spectral Characterization of Noncollinear Optical Parametric Amplifiers," presented at *Advanced Solid-State Photonics*, paper AME5, San Diego, CA (2010)

[6] S. Wielandy, 'Implications of higher-order mode content in large mode area fibers with good beam quality,' Opt. Express **15**, 15402 (2007).

[7] P. Le Boudec, *et al*, 'Self-pulsing in Er^{3+}-doped fiber laser', Opt. Quantum Electron., **25**, 359, (1993).

[8] F. Brunet, *et al.* 'A Simple Model Describing Both Self-Mode Locking and Sustained Self-Pulsing in Ytterbium-Doped Ring Fiber Lasers,' J. Lightwave Technol. **23**, 2131 (2005)